EDGE ARTICLE

Check for updates

Boosting the ORR performance of modified carbon black *via* C–O bonds†

Chen Ouyang, Bing Ni, [iD] Zhaoyang Sun, [iD] Jing Zhuang, Hai Xiao [iD] * and Xun Wang [iD] *

In the research into oxygen reduction reaction (ORR) catalysts that are applicable to proton exchange membrane fuel cells (PEMFCs), many efforts have been made over a long time period to increase the catalytic activity and reduce the cost. Conductive carbon black is a type of load material widely used in industry. We have developed a cheap carbonization method using Co^{2+}, Zn^{2+} and 2-methylimidazole (2-MI) on the surface of carbon black. The modified carbon black (MCB) catalyst with high ORR activity has a large diffusion-limited current density (MCB-3 6.18 mA cm^{-2}), a half-wave potential (MCB-3 0.858 V), and no obvious decay after 20 000 cyclic voltammetry cycles. The characterization and controlled experiment results show that the metal content in the MCB is very low, even though it cannot be detected using extended X-ray absorption fine structure spectroscopy (EXAFS), and its ORR activity may be related to the formation of C–O bonds on the surface during the modification process. Subsequent density functional theory calculation results also support this idea. Through the simple modification of carbon black, a catalyst with excellent performance and low price can be obtained. At the same time, the study of the active site of the C–O bond will also provide new ideas for the study of ORR catalysts.

Introduction

The oxygen reduction reaction (ORR) has important applications in advanced energy conversion technologies, including proton exchange membrane fuel cells (PEMFCs) and batteries. ORR is kinetically slow and requires a catalyst (usually Pt/C). Moreover, the prohibitive cost and scarcity of Pt limits the commercialization of PEMFCs. In order to address these issues, a large number of inexpensive high activity and superior stability alternatives have been recently been investigated as substitutes for Pt-only catalysts.[1–3] Among them, carbon-based nonprecious metal nanocatalysts (NPMNs) with a porous structure are seen as one of the most promising ORR catalysts with a low cost and high raw material abundance.[4–6] Its porous structure can provide a large number of exposed active sites such as metal oxide nanoparticles, metal–N$_4$ complexes and metal–C–N moieties, enhanced accessibility of reactants, fast mass transport and electron transfer. These all contribute towards improving the catalytic performance.

Metal–organic frameworks (MOFs) comprise ordered connections between metal centers and organic ligands.[7,8] MOF-derived NPMNs have been demonstrated to have great potential in ORR electrocatalysis, serving as catalysts or

supports.[9–12] Compared with traditional NPMNs synthesis, MOFs can be developed by choosing different metal ions and ligands to easily obtain different framework structures.[12–15] In addition, the surface area and pore structure of MOFs can be retained in NPMNs to varying extents by controlling the pyrolysis and after treatment to provide suitable surface properties and microstructure. Usually, pyrolyzed MOFs contain S, N heteroatoms from the ligand, and many studies have shown that the doping of S, N atoms is the key to the ORR catalytic performance of NPMNs. However, a large number of C–O functional groups are contained in NPMNs and these also serve as sources of ORR activity. In our previous work,[16] we prepared a carbon black catalyst loaded with a trace amount (≈ 5 wt%) of Co_3O_4 particles by successively soaking carbon black[17] in a solution of cobalt nitrate and 2-methylimidazole (2-MI). However, in a further treatment, we removed the metal particles on the surface of the material by immersion in acidic solution, and the catalytic activity of the ORR of the treated material was further enhanced, indicating that the excellent catalytic activity of this type of material may not be related to the metal.

Here, we have devised a novel method of modifying carbon black. The modified carbon black (MCB), produced by high-temperature carbonization after treating carbon black with Co^{2+} and 2-MI under the control of Zn^{2+}, has high ORR activity, long durability, and resistance to methanol poisoning. Vulcan XC72 (VXC72) is an economical form of conductive carbon black (about $0.5 per kg). We treated the carbon black with a small number of metal ions and ligands and then calcined it. The

Key Lab of Organic Optoelectronics and Molecular Engineering, Department of Chemistry, Tsinghua University, Beijing 100084, China. E-mail: wangxun@mail.tsinghua.edu.cn; haixiao@tsinghua.edu.cn

resulting MCB showed markedly improved ORR activity compared with that before modification, and exhibited an excellent half-wave potential ($E_{1/2}$) and diffusion-limiting current density (J_L). Its stability and resistance to methanol poisoning were also impressive. At the same time, the catalytic activity of the MCB could be positively correlated to its C–O bond content, and subsequent density functional theory (DFT) calculations also supported this conclusion. These findings provide strong evidence for the clarification of the oxygen reduction catalytic activity of carbon materials and provide theoretical guidance for the subsequent preparation of oxygen reduction catalysts for carbon materials.

Results

Synthesis and characterization of the MCB

In a typical synthesis (Fig. S1, for details see the ESI†), carbon black was poured into a container filled with cobalt nitrate and zinc nitrate in ethanol and dispersed *via* sonication. The mixture was stirred with 2-MI in ethanol for 12 hours. The reaction of Co^{2+} and 2-MI to generate zeolitic imidazolate framework (ZIF)-67 is fast and the particle size is large. It is hard to form an even layer of the ZIF on the surface of carbon black without control. Here, we added a certain amount of Zn^{2+}, which reacts with 2-MI to generate ZIF-8. This reaction is slow, and it is difficult to generate large particles in ethanol.

The addition of the materials in this competitive reaction can be used to effectively control the speed of the reaction between Co^{2+} and 2-MI in order to obtain the desired precursor (Fig. 1a). PXRD measurements confirmed the existence of the ZIF (Fig. S2†). The obtained precursor was pyrolyzed in a furnace at 800 °C for 2 hours under the protection of nitrogen to obtain the MCB. In general, the pyrolysis of a ZIF under gas protection generates nitrogen-doped nanoporous carbon containing metal particles. From transmission electron microscopy (TEM) measurements (Fig. 1b), it can be seen that the surface structure of the MCB is very similar to that of the original

carbon black (Fig. S3†), with no obvious particles, and the scanning transmission electron microscopy (STEM) images (Fig. 1b) also reflect this. Energy dispersive spectroscopic (EDS) elemental analysis results (Fig. 1c) show that the structure is mainly composed of O embedded in a carbon substrate and only trace amounts of cobalt and zinc were detected by EDS.

ORR performance and surface chemistry

Then we tested the ORR performance of the MCB in alkaline solution. Cyclic voltammetry (CV) was carried out in N_2-saturated and O_2-saturated solutions, respectively, to prove that the ORR occurred within the tested potential range and the capacitance was found to be very low over the tested range. The linear sweep voltammetry (LSV) curves (Fig. 2a) show that the ORR catalytic activity of the MCB was greatly improved compared with that of the original carbon black, with an onset potential ($E_{on\ set}$) increase from 0.824 V to 0.937 V, a half-wave potential ($E_{1/2}$) increase from 0.73 V to 0.858 V, and a diffusion-limiting current density (J_L) increase from 4.84 mA cm^{-2} to 6.18 mA cm^{-2}. These three MCB values are also better than those of commercial Pt/C ($E_{on\ set}$ = 0.958 V, $E_{1/2}$ = 0.842 V, J_L = 5.40 mA cm^{-2}), which shows excellent ORR catalytic activity, and the current induced by the capacitance of the catalyst was found to be low.[18]

LSV curves at different rotation speed were obtained by adjusting the rotation speed of the rotating disk electrode and the corresponding LSV plots were recorded (Fig. 2b). Then, the electron transfer number of the catalytic reaction was obtained using the Koutecky–Levich (K–L) equation. The fitted lines suggested that when the value in the wide range was almost 4, O_2 was reduced to H_2O rather than H_2O_2, which may corrode the catalysts and lead to failure in applications.

In the meantime, we also evaluated the anti-methanol poisoning properties of MCB (Fig. 2c) and its stability under
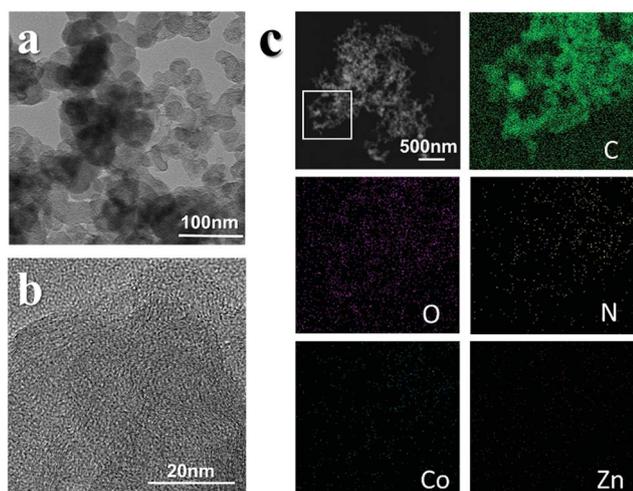

Fig. 1 (left) TEM images of the precursor (a) and TEM images of the MCB (b). (right) EDS mapping results of the MCB (c).
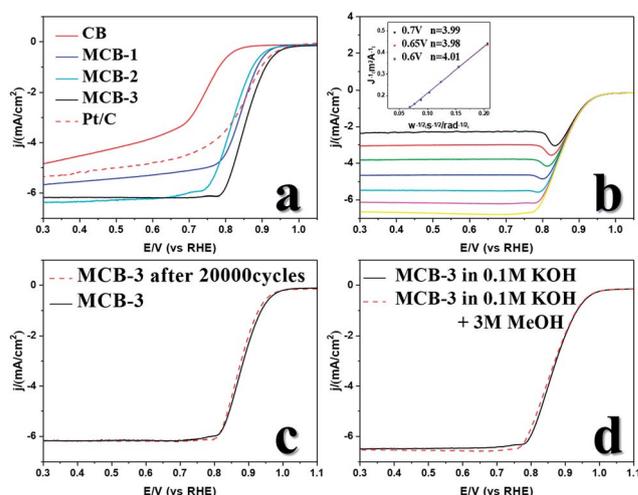

Fig. 2 (a) LSV curves of the MCB and other comparable catalysts in 0.1 M KOH. (b) LSV curves of MCB-3 at different rotating speeds of the rotating disk electrode. The inset of (b) shows the K–L plot of MCB-3 at various potentials. (c) LSV curves of the pristine sample and the sample after 20 000 ADT cycles. (d) LSV curves of MCB-3 in 0.1 M KOH solution with and without 3 M methanol solutions.

long-term test conditions (Fig. 2d). When we added 3 M methanol to a 0.1 M KOH solution in the LSV measurements, hardly any change was observed in the curve. In addition, an accelerated durability test (ADT) at a scan rate of 100 mV s^{-1} in the range of 0.6–1.1 V was used to evaluate the stability of the MCB. The LSV plot after 20 000 ADT cycles showed no obvious change compared to that of the original LSV curve, suggesting good stability.

It is generally believed that during the pyrolysis of ZIF into nanoporous carbon, metal ions are reduced to metal nanoparticles that can catalyze the graphitization of the imidazole framework[19,20] and also react with nitrogen in the organic ligand to form an MN$_x$ structure,[21] to produce a final carbonized nitrogen-doped nanoporous carbon material containing metal nanoparticles or made up of an MN$_x$ composite structure.[22] Metal oxide nanoparticles,[23] metal–N$_4$ complexes and metal–C–N moieties all function independently as active centers,[24] but it is not known which of these centers is best for ORR.

The precursor to the MCB pyrolysis was carbon black, that grew a thin layer of ZIF on the material surface,[25] however, we did not observe metal nanoparticles or an MN$_x$ composite structure using characterization techniques such as TEM and EDS mapping of the MCB. We used inductively-coupled plasma mass spectrometry (ICP-MS) to analyze the metal content in the MCB and the detectable Co content was 0.27% and the Zn content was 0.05%. This extremely low content indicates that if the Co acts as an ORR active center in the MCB,[26] it can only exist as single atomic site Co.[27] However, the results of extended X-ray absorption fine structure (EXAFS) measurements (Fig. 3a) indicated that the trace amount of cobalt present in the MCB was in the form of tricobalt tetraoxide. We calculated the Co content and performance (expressed as a half-wave potential, $E_{1/2}$) of some MCB materials (Fig. 3b).

The results show that there is no discernible correlation between the Co content and catalytic activity.[28] We also tried to treat MCB with a small amount of acid. Its catalytic performance was found to be similar to that of untreated MCB (Fig. 3b). The obtained MCB-H was analyzed by ICP-MS and EXAFS (Fig. S13†). The ICP-MS results showed that the Co content was 0.05%, and the peak for Co was not observed in the results of EXAFS. On the other hand, we tested the Co poisoning

by adding 0.05 M KSCN to a 0.1 M KOH solution. The results (Fig. S15†) show that the addition of SCN$^-$ had no significant effect on the catalytic activity of the MCB. Combined with previous TEM characterization results, we believe that elemental cobalt is formed by the hydrolysis of cobalt ions during the preparation of the precursor and is not involved in the ORR activity.

In order to gain a better understanding of the catalytic activity of MCB, we prepared numerous different MCB materials by controlling the preparation conditions, characterized them and tested their electrochemical performance (Fig. S4, Tables S1 and S2†).

MCB-1 and MCB-2 were prepared by controlling the zinc nitrate, cobalt nitrate and 2-MI ratio (Zn : Co : MI) of the precursor mixture (for details see the ESI†). They were found to have excellent oxygen reduction catalytic activity (Fig. 2a), with half-wave potentials of 0.842 V and 0.819 V, lower than that of MCB-3, and the Tafel slopes for MCB-1, 2 and 3 were observed to be very similar, all at around 60 (Fig. S10†). TEM images (Fig. S5†) and X-ray photoelectron spectra (XPS) showed that their morphologies were very similar to that of MCB-3 and carbon black, but their XPS under synchrotron radiation results (Fig. S6†) showed significant differences. The results of the XPS showed that only C and O peaks were clearly observed in all four materials, including carbon black, which further proves that there is only effective doping in the carbon black. The C 1s peaks are composed of three peaks (Fig. 4a), which can be attributed to the presence of C=C, C–O and COO bonds. The O 1s peak is also comprised of three peaks (Fig. 4b), which could arise from C–O, COO and adsorbed oxygen and carbon dioxide. It can be seen that in the C 1s spectrum, the peak intensities of C=C decrease in the order of VXC72, MCB-1, MCB-2 and MCB-3, and the intensities of the C–O peaks increase in turn. Correspondingly, the peak intensity of C–O also increased in the order of VXC72, MCB-1, MCB-2 and MCB-3. There was no significant change observed in the peak intensity of COO and adsorbed oxygen and carbon dioxide. By calcining the materials at 980 °C and examining the exhausted gas we were able to determine the exact amount of C, O, and N. The results (Table S3†) showed that the O content increased from the VXC72 sample to MCB-3.
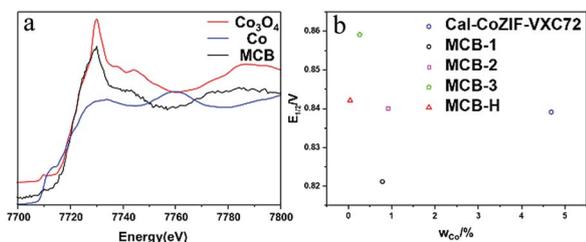

Fig. 3 (a) XANES spectra of MCB, Co$_3$O$_4$, and Co foil. The MCB and Co$_3$O$_4$ are very similar. (b) $E_{1/2}$-w_{Co} diagram, where MCB-H represents acid treated MCB-3, and Cal-CoZIF-VXC72 is a carbon material from our previous work. It can be seen that there is no obvious correlation between the Co content of the catalyst and its performance.
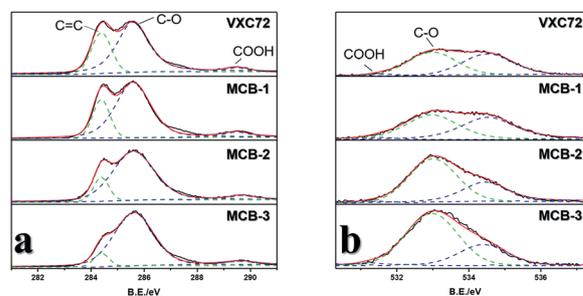

Fig. 4 (a), (b) XPS survey spectra under synchrotron radiation and (a) high-resolution C$_{1s}$ scans of MCB-1, MCB-2, MCB-3 and VXC72. (b) High-resolution O$_{1s}$ scans of MCB-1, MCB-2, MCB-3 and VXC72. The dashed lines indicate the fitted peaks.

The above results show that during modification of carbon black, a large number of C=C bonds were oxidized to C–O bonds on the surface of carbon black, and the catalytic activity of the material was significantly enhanced upon an increase in the O content. To illustrate the effect of the oxidation process on carbon black ORR activity, we treated the carbon black briefly with 1 M HNO_3. The treated carbon black showed considerably better ORR activity than untreated carbon black, but not as good as that of MCB-1, 2, and 3 (Fig. S7†). This is probably due to all of the MCB samples containing a certain amount of nitrogen (Table S3†), but the amount of N is much lower than in the N-doped carbon materials reported in the literature (around 9% (ref. 1)), and this content could not be significantly correlated with the differences in catalytic activity between MCB 1, 2 and 3. Therefore, the nitrogen in the material has an impact on the catalytic activity but is not the most important factor in the MCB material activity.

From this, we speculate that during pyrolysis, the metal ions originally adsorbed on the surface of the carbon black in the ZIF microstructure are reduced to metal particles by carbon black, while the metal particles catalyze the graphitization of the ZIF structure.[29] However, due to the size of the ZIF microstructure adsorbed on the surface of the carbon black, the metal particles are produced near the surface. After catalyzing the ZIF graphitization, the metal particles are vaporized and volatilized at 800 °C. Therefore, there were no significant differences between the TEM images of the MCB and carbon black, with no metal particles on the surface.

At the same time, the graphitization process of the ZIF changed the surface structure of the carbon black, so that some of the C=C bonds were converted into C–O bonds. This transformation greatly enhanced the catalytic activity of the carbon black in the ORR and also showed that the active center is the C–O bond.

The above experimental results show that the MCB contains a large number of oxygen functional groups that regulate the electronic structure of the carbon black and significantly increase its oxygen reduction catalytic activity. Next, we used DFT calculations to further explain the effect of the oxygen-containing functional groups on the catalytic activity.

The binding ability of the active sites of the material and the ORR intermediate determine the catalytic activity to a large extent. For a carbon material with a graphite structure, the active center is the chair edge, so the more stable chair edge helps to generate more active sites and thus enhances the catalytic activity.

DFT calculations

For theoretical modeling, we employed approximate models of carbon black based on the graphene oxide structure, which features oxygen-containing functional groups on its basal planes. Previous characterization results showed that the number of C–O bonds in the MCB greatly increased. Based on this, we established models of carbon black (Fig. 5a) and MCB (Fig. 5b) armchair edges with different O content surface structure models.[17,30] The calculations showed that the
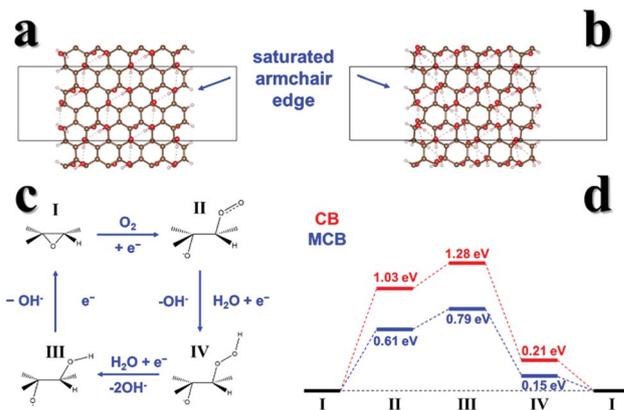

Fig. 5 Models of the armchair edges of (a) carbon black and (b) MCB. (c) Predicted ORR mechanism on the armchair edges of carbon black and MCB. (d) The ORR free energy profiles, which show that additional OH groups in MCB stabilize the ORR intermediates.

armchair edge free energy of the MCB is −0.31 eV per edge site, more stable than that of CB at 0.03 eV per edge site, and thus MCB has more exposed active sites.

We further identified the most stable adsorption sites on the armchair edges and then optimized the intermediates to predict the ORR mechanism. In our predicted mechanism (Fig. 5c), O_2 is chemisorbed to the edge epoxide site, and reduced to hydroxide accompanied by epoxide ring opening and closing that completes the catalytic cycle.[31] Our calculations clearly show that the required free energy input of ORR catalyzed by MCB is lower than that of carbon black.

Thus, our DFT results confirm that further oxidation (MCB) of CB increases the ORR activity, and that there are two contributing factors. (1) The active armchair edge is stabilized and more active sites can be generated; (2) the additional OH groups produced by further oxidation can stabilize the ORR intermediates.

The good activity, stability, and easy preparation of MCB show that it is a promising material that can be used in future applications. We also sought to further enhance the activity or further simplify the synthetic procedures, but it seems that as-prepared MCB-3 is the most suitable material for real applications. By pre-treating the carbon black and changing the solvent (for details see the ESI†), we grew a layer of ZIF on the surface of the carbon black (Fig. S8†). After the same carbonization treatment, we obtained MCB-4. However, when the ZIF size was large, there was a decrease in the catalytic activity. This may be due to a decrease in the size of the ZIF that led to a decrease in the modification of the carbon black during the ZIF carbonization. If more interferences, such as sonication or stirring, were employed during the synthesis, there was a decrease in the activity[32] (Fig. S9†). Other methods to reduce the costs were further studied. For example, $Co(NO_3)_2$ and 2-MI solutions could be reused in the next batch. Considering its simplicity and activity, MCB could be a more promising material for use in applications than other comparable catalysts.

Conclusions

In summary, we developed a simple method to modify commercial carbon black to obtain MCB with a high ORR activity and stability that can be prepared at a low cost. At the same time, we demonstrated that the ORR activity of the MCB prepared in this method is derived from the carbon black itself. Nanoporous carbons produced by ZIF carbonization make up a common class of ORR catalytic materials. However, they generally have the disadvantage of poor conductivity, which limits their utility in electrocatalytic reactions. Carbon black (VXC72) has excellent electrical conductivity. Electrochemical test results also show that the MCB has better catalytic performance than the general ZIF pyrolysis products. We also studied in detail the sources of the ORR activity of MCB and together with the results of XPS characterization and DFT calculations, it was proven that the active carbon source of the MCB is the modified CO bonds on the carbon substrate. This discovery shows that we can use a very inexpensive method to obtain a large number of excellent catalytically active sites in a material. The catalyst with carbon black as an active center has a wide range of sources and is simple to prepare and highly reproducible, which greatly reduces the production cost and has good prospects for application. At the same time, the establishing of the active center also provides a research idea for the modification of the ORR catalytic activity of carbon black in alkaline environments.

Conflicts of interest

There are no conflicts to declare.

Acknowledgements

Notes and references

1 W. Xia, C. Qu, Z. Liang, B. Zhao, S. Dai, B. Qiu, Y. Jiao, Q. Zhang, X. Huang, W. Guo, D. Dang, R. Zou, D. Xia, Q. Xu and M. Liu, *Nano Lett.*, 2017, **17**, 2788–2795.

2 W. Gang, Y. Ce, Z. Wanpeng, L. Qianru, W. Ning, L. Tao, Z. Hua, C. Hangrong and S. Jianlin, *Adv. Mater.*, 2017, **29**, 1703436.

3 B. Y. Guan, L. Yu and X. W. Lou, *Energy Environ. Sci.*, 2016, **9**, 3092–3096.

4 T. Cheng and Z. Qiang, *Adv. Mater.*, 2017, **29**, 1604103.

5 Z. Lu, W. Xu, J. Ma, Y. Li, X. Sun and L. Jiang, *Adv. Mater.*, 2016, **28**, 7155–7161.

6 X. Liu and L. Dai, *Nat. Rev. Mater.*, 2016, **1**, 16064.

7 M. Hu, J. Reboul, S. Furukawa, L. Radhakrishnan, Y. Zhang, P. Srinivasu, H. Iwai, H. Wang, Y. Nemoto, N. Suzuki, S. Kitagawa and Y. Yamauchi, *Chem. Commun.*, 2011, **47**, 8124–8126.

8 R. R. Salunkhe, C. Young, J. Tang, T. Takei, Y. Ide, N. Kobayashi and Y. Yamauchi, *Chem. Commun.*, 2016, **52**, 4764–4767.

9 B. P. Setzler, Z. Zhuang, J. A. Wittkopf and Y. Yan, *Nat. Nanotechnol.*, 2016, **11**, 1020–1025.

10 R. R. Salunkhe, Y. V. Kaneti, J. Kim, J. H. Kim and Y. Yamauchi, *Acc. Chem. Res.*, 2016, **49**, 2796–2806.

11 W. Chaikittisilp, N. L. Torad, C. Li, M. Imura, N. Suzuki, S. Ishihara, K. Ariga and Y. Yamauchi, *Chemistry*, 2014, **20**, 4217–4221.

12 J. Tang and Y. Yamauchi, *Nat. Chem.*, 2016, **8**, 638–639.

13 W. Xia, A. Mahmood, Z. Liang, R. Zou and S. Guo, *Angew. Chem., Int. Ed.*, 2016, **55**, 2650–2676.

14 W. Zhang, X. Jiang, Y. Zhao, A. Carne-Sanchez, V. Malgras, J. Kim, J. H. Kim, S. Wang, J. Liu, J. S. Jiang, Y. Yamauchi and M. Hu, *Chem. Sci.*, 2017, **8**, 3538–3546.

15 L. Radhakrishnan, J. Reboul, S. Furukawa, P. Srinivasu, S. Kitagawa and Y. Yamauchi, *Chem. Mater.*, 2011, **23**, 1225–1231.

16 N. Bing, O. Chen, X. Xiaobin, Z. Jing and W. Xun, *Adv. Mater.*, 2017, **29**, 1701354.

17 O. B. Berryman, A. C. Sather, B. P. Hay, J. S. Meisner and D. W. Johnson, *J. Am. Chem. Soc.*, 2008, **130**, 10895–10897.

18 B. Y. Xia, Y. Yan, N. Li, H. B. Wu, X. W. Lou and X. Wang, *Nat. Energy*, 2016, **1**, 15006.

19 Z. Wei, J. Xiangfen, W. Xuebin, K. Y. Valentino, C. Yinxiang, L. Jian, J. Ji-Sen, Y. Yusuke and H. Ming, *Angew. Chem., Int. Ed.*, 2017, **56**, 8435–8440.

20 S. Lu, Y. Huijun, H. Xing, B. Tong, S. Run, Z. Yufei, G. I. N. Waterhouse, W. Li-Zhu, T. Chen-Ho and Z. Tierui, *Adv. Mater.*, 2016, **28**, 1668–1674.

21 J. H. Zagal and M. T. Koper, *Angew. Chem., Int. Ed.*, 2016, **55**, 14510–14521.

22 D. Guo, R. Shibuya, C. Akiba, S. Saji, T. Kondo and J. Nakamura, *Science*, 2016, **351**, 361–365.

23 C. Young, J. Wang, J. Kim, Y. Sugahara, J. Henzie and Y. Yamauchi, *Chem. Mater.*, 2018, **30**, 3379–3386.

24 J. Zhang, Z. Zhao, Z. Xia and L. Dai, *Nat. Nanotechnol.*, 2015, **10**, 444–452.

25 C. Yu-Zhen, W. Chengming, W. Zhen-Yu, X. Yujie, X. Qiang, Y. Shu-Hong and J. Hai-Long, *Adv. Mater.*, 2015, **27**, 5010–5016.

26 Y. Liang, Y. Li, H. Wang, J. Zhou, J. Wang, T. Regier and H. Dai, *Nat. Mater.*, 2011, **10**, 780.

27 H. Aijuan, C. Wenxing, Z. Shaolong, Z. Maolin, H. Yunhu, Z. Jian, J. Shufang, Z. Lirong, W. Yu, G. Lin, C. Chen, P. Qing, W. Dingsheng and L. Yadong, *Adv. Mater.*, 2018, **30**, 1706508.

28 Y. Peiqun, Y. Tao, W. Yuen, Z. Lirong, L. Yue, L. Wei, J. Huanxin, Z. Junfa, H. Xun, D. Zhaoxiang, Z. Gang, W. Shiqiang and L. Yadong, *Angew. Chem., Int. Ed.*, 2016, **55**, 10800–10805.

29 C. Niu, J. Meng, X. Wang, C. Han, M. Yan, K. Zhao, X. Xu, W. Ren, Y. Zhao, L. Xu, Q. Zhang, D. Zhao and L. Mai, *Nat. Commun.*, 2015, **6**, 7402.

30 Z. Lu, G. Chen, S. Siahrostami, Z. Chen, K. Liu, J. Xie, L. Liao, T. Wu, D. Lin, Y. Liu, T. F. Jaramillo, J. K. Nørskov and Y. Cui, *Nat. Catal.*, 2018, **1**, 156–162.

31 G.-L. Chai, M. Boero, Z. Hou, K. Terakura and W. Cheng, *ACS Catal.*, 2017, **7**, 7908–7916.

32 S. Rojas-Carbonell, K. Artyushkova, A. Serov, C. Santoro, I. Matanovic and P. Atanassov, *ACS Catal.*, 2018, **8**, 3041–3053.